Kinetic interpretation of hepatic multiple-indicator dilution studies

C. A. Goresky

Am J Physiol Gastrointest Liver Physiol 245:G1-G12, 1983. ;

AJP - Gastrointestinal and Liver Physiology publishes original articles pertaining to all aspects of research involving normal or abnormal function of the gastrointestinal tract, hepatobiliary system, and pancreas. It is published 12 times a year (monthly) by the American Physiological Society, 9650 Rockville Pike, Bethesda MD 20814-3991. ISSN: 0193-1857, ESSN: 1522-1547. Visit our website at http://www.the-aps.org/.

Kinetic interpretation of hepatic multiple-indicator dilution studies

CARL A. GORESKY
McGill University Medical Clinic, Montreal General Hospital and Departments of Medicine and Physiology, McGill University, Montreal, Quebec HG3 1A4, Canada

GORESKY, CARL A. *Kinetic interpretation of hepatic multiple-indicator dilution studies.* Am. J. Physiol. 245 (Gastrointest. Liver Physiol. 8): G1–G12, 1983.—The single-injection, multiple-indicator dilution approach, together with an analysis based on a model of microcirculatory events, provides a way of determining the composition of and the rates of processes in the liver. By comparison with a vascular reference, labeled red cells, a set of interstitial materials are found to enter the Disse space in a delayed-wave, flow-limited fashion, larger materials being excluded from a proportion of the space, and labeled water is found to undergo flow-limited distribution into the liver cells. In contrast, many other substances exhibit barrier-limited exchange with the liver cells; their tracer outflow profiles consist of throughput material (which has entered the interstitium but not the liver cells) and of returning material (which has entered the cells, later to return to the vascular space). Intracellular metabolic sequestration or biliary secretion reduces the outflow recovery of returning tracer; it also results in decreasing steady-state concentrations along sinusoids and cells and, where the cell membrane is limiting, in a step-down in concentration across it.

flow-limited distribution; excluded-volume effects; membrane carrier transport; barrier limitation; intracellular metabolic sequestration; sinusoidal and cellular axial concentration gradients; protein binding; cellular binding proteins; hepatic glucose exchange; hepatic galactose uptake; hepatic bilirubin uptake

THE LIVER is uniquely designed to interact with the blood perfusing it. Blood perfuses the sinusoids on either side of each hepatic cell plate, flowing concurrently from input to output. The lining sinusoidal endothelium is perforated by multiple fenestra, so that molecules dissolved in the plasma phase of blood gain immediate access to the interstitium, the space of Disse. Beyond this space lies the first concrete barrier in the system, the multivillous sinusoidal surface of the liver parenchymal cells. This cell membrane is the only barrier interposed between plasma and the intracellular metabolic machinery. It has permeability properties much like those of other cells; it is highly permeable to labeled water, impermeable to sucrose and most large protein molecules, and has specific nonlinear permeability properties for a variety of important metabolic substrates (the entry mechanisms for some of these fulfill the criteria of carrier-mediated membrane transport). Intracellular metabolic sequestration or removal of substrate behind the barrier leads to a step-down in concentration across the membrane, so that intracellular concentrations of substrate are lower in the cells than in the plasma at a parallel position; because of the distributed-in-space character of the hepatic acinus, the removal creates a set of steady-state axial (in the direction of flow) gradients in substrate concentration, in both sinusoids and liver cells. The kinetics underlying intracellular consumption processes are also generally nonlinear, being epitomized by Michaelis-Menten kinetics.

These phenomena are best studied in the intact liver in vivo (17). Here the distributed-in-space character of the hepatic acinus is important: downstream cells receive both material that has failed to enter upstream cells and material that has entered these cells but later returned to the circulation. For most important metabolic substrates, it is impossible to examine kinetic or even concentration phenomena directly; thus an indirect approach has had to be developed. The use of tracer transients (that is, the interpretation of outflow tracer patterns, knowing the pattern of trace input) has proved to be the most productive of the indirect methods for defining kinetic processes within the organ. This approach takes into account not only time-dependent effects but also the distributed-in-space character of events within the hepatic acinus. It provides a realistic alternative to the too simple lumped compartmental description of the liver classically utilized in pharmacokinetics.

Finding Tracer References for Cell Entry Processes

The indirect approach developed to investigate cell entry and sequestration in the whole organ is the multiple-indicator dilution technique (6). In this approach, a tracer for the substance to be studied and an appropriate reference tracer are injected together into the blood flowing into an organ; serial outflow samples are ana-

An introduction by E. L. Forker and the first three articles in this series entitled "Hepatic Transport Kinetics" appeared in the June issue of the journal.

lyzed for their contained activity; and outflow dilution curves are constructed from the results of the analysis. To provide a framework such that each curve can be directly compared with another, the outflow concentration of each tracer is divided by the total injected; this provides a normalized value, an outflow fraction per milliliter.

In organs with a continuous capillary lining, the exchange rates for labeled albumin are so low that a perceptible amount does not leave the vasculature during a single passage. Labeled albumin is then an appropriate reference for the transcapillary passage of materials dissolved in the plasma phase of blood. In the liver, however, its behavior was initially less well defined. Goresky (9) carried out a set of indicator dilution studies in the liver in which labeled red cells, labeled albumin, labeled sucrose and sodium (classic extracellular references), and labeled water (which would be expected to penetrate liver cells freely) were included in the injection mixture. The outflow curves from one such study are illustrated in Fig. 1. The labeled red cells emerge first; the curve depicting their outflow fraction per milliliter reaches the earliest and highest peak and decays most quickly. The extracellular substances (which are dissolved in the plasma phase) show a progressive delay in their outflow appearance, diminution in and delay in reaching their peak, and a progressively decreasing rate of downslope decay. The curves appear to form a continuous family. The phenomena shaping the most displaced curve of the group, labeled water, appear similar to those affecting the intermediate sets of curves.

These data can be interpreted only by the use of mathematical modeling. In terms of the physical quantities involved, the modeling must also be sensible. Goresky (9) carried out a dimensional analysis of expected diffusional equilibration rates within tissue sheets with a depth corresponding to that of the space of Disse (the interstitium), a liver cell half width, and the axial length of a sinusoid. Diffusional equilibration over the first two dimensions was estimated to be complete within an interval that was a miniscule fraction of a red cell transit time, whereas the diffusional equilibration across distances corresponding to the length of a sinusoid was calculated to require times several orders of magnitude larger than a sinusoidal transit time. The expectations arising from this dimensional analysis were incorporated into a distributed-in-space model of diffusional exchange at the level of the sinusoids, in the absence of a barrier. A bolus of diffusible material, carried along by flow, was envisaged to exchange with an adjacent interstitial compartment; because of the extraordinary rapidity of diffusional equilibration across dimensions of the order of the interstitium, it was assumed that equilibration within this space, transverse to the flow, occurred virtually instantaneously. A delayed-wave, flow-limited model resulted. In this kind of model the bolus of diffusible material behaves as though it were traveling in its total space of distribution; as a result it travels slower, emerging at the outflow later than a reference carried along by flow (a labeled red cell). The sinusoidal transit time of the diffusible label is increased by the ratio of its total-to-accessible sinusoidal vascular space.

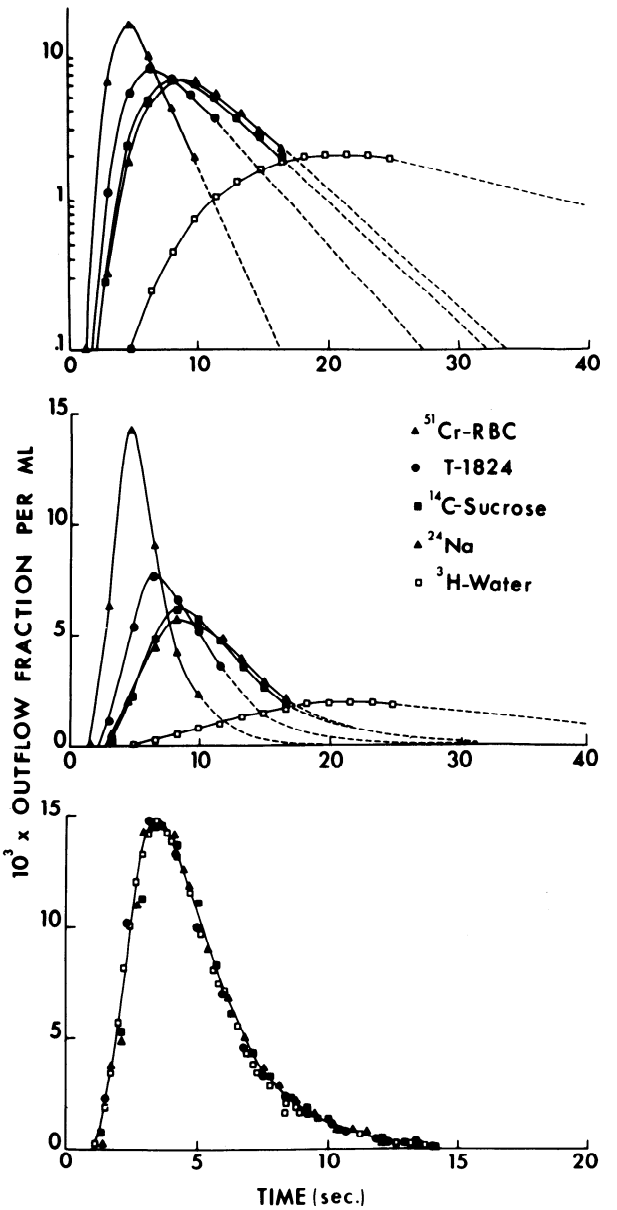

FIG. 1. Normalized hepatic venous dilution curves. T-1824 refers to albumin labeled with Evans blue dye. Ordinate scale in upper panel is logarithmic and that in middle panel, linear. Extrapolations carried out to exclude recirculation are indicated with dashed lines. Superimposition of adjusted diffusible label curves on labeled red cell curve is illustrated in bottom panel. Time scale has been adjusted for input and output catheter transit times. [Reprinted with permission from *Federation Proceedings* (19).]

The injected tracers pass through both large and small vessels. It is assumed that no displacement occurs between reference intravascular and diffusible tracers in the large vessels: it all occurs in the exchanging vessels. The interrelations between whole-organ outflow reference and diffusible tracer curves will depend not only on the phenomena occurring within each sinusoid but also on the way the transit times in larger vessels and sinusoids are interrelated. Various combinations are possible, depending on the structure of the network and the kind of flow coupling in the system. The pattern corresponding to the liver was found to lie at a simple extreme in this possible spectrum (20, 26). The distribution of out-

flow transit times was found to correspond to the distribution of sinusoidal transit times; the distribution of transit times in large vessels was so compact that a single value could be assumed. Thus it was possible to derive a test for the single-sinusoid modeling. If, after a common transit time in large vessels, the sinusoidal transit time for each diffusible label in the liver is increased by the ratio of its total-to-accessible sinusoidal vascular space, then it should be possible to reverse this flow-limited delay effect in the curve for each diffusible label. Decreasing the sinusoidal transit times of each diffusible label by the inverse of its appropriate ratio (and increasing the outflow fraction per milliliter by that ratio to preserve the area under the curve) should result in superimposition of the whole group of diffusible tracer curves on the vascular reference-labeled red cell curve. This occurs (see, for example, lower panel of Fig. 1). The adjusted curves for the extracellular substances and even that for labeled water uniformly superimpose on the curve for the labeled red cells. By this criterion, all of these undergo flow-limited distribution, the extracellular substances into the interstitium and the labeled water into both interstitium and liver cells, during their passage along the sinusoid.

Labeled albumin, inulin, and sucrose, although all extracellular in their distribution, occupy successively increasing interstitial volumes. Exclusion of inulin and albumin from part of the interstitial space is evident (inulin enters only 0.87 of the sucrose-accessible space and albumin, 0.65 of this space). Labeled sodium occupies essentially the same space as labeled sucrose. Because of the anatomic characteristics of the liver microvasculature, the interstitium is freely exposed to probes in the plasma. Consequently the liver was the first organ in which the exclusion properties of the interstitium were demonstrated in vivo (9).

This study provides a set of guideposts describing the behavior of materials entering the interstitium; with this background, it becomes possible to approach events at the cell membrane.

Barrier-Limited Exchange Between Liver Cells and Plasma

The next challenge is to describe the entry into and efflux from the liver of tracer materials not consumed or removed by the liver. This kind of study should be designed so as to minimize the degree of uncertainty involved in defining the behavior of the substance under study (the maximum amount of experimentally applicable data must be obtained; this reduces the amount of information that must be produced by modeling). The inference is that, in any examination of materials entering cells, the knowledge gained from the study of the group of interstitial materials should be utilized; the study should therefore include, as a second reference, a diffusible substance that behaves exactly like the substance under study except for its penetration of the cell membrane and distribution into the liver cells. The second reference should ordinarily be distributed in blood in the same fashion as the substance under study, and it should have the same kind of partitioning in the interstitial space as the substance under study. For materials tightly bound to albumin, labeled albumin is an appropriate second reference; for materials of lower molecular weight confined to the plasma phase of blood, which enter essentially all of the interstitial space, labeled sucrose is an appropriate reference.

A second inference also comes from the study of the compartment materials. Because the behavior of both the no-entry (cell-membrane-impermeable, second-reference group) and the infinitely permeable cell-entry (labeled water) materials has been characterized in the initial experimental and modeling studies, it is possible to explore intermediate permeating cases experimentally and, with a model converging on the two asymptotes, to analyze the data with confidence. It is possible to utilize both the early parts of the tracer curve (which are expected, in low-permeability cases, to consist chiefly of tracer that has traversed the circulation without entering the liver cells) and the later parts of the curve (which are composed of tracer that has entered the cells, to later return to the circulation) in the analysis. It is not necessary to adopt the Crone approach (7), in which an influx permeability-surface product is approximated by use of a limited part of the data (the upslopes of reference and tracer substrate curves) and for which the useful range is confined to the low-permeability end of the spectrum. Instead, with a model of cellular exchange encompassing the two permeability extremes (which is also useful at the higher end), all the data obtained in the upslope, peak, and downslope parts of the tracer substrate curve will be able to be used in the analysis. In the modeling, material in the interstitium is visualized as exchanging with adjacent liver cells at each point along the length. In fitting outflow data, the permeability-surface product of the cell membrane can be varied from low to high, so as to encompass the two ends of the spectrum. Influx and efflux parameters and relative liver cellular space sizes can be estimated and the behavior of both low- and high-permeability substances explored.

The biological behavior of the system must also be taken into account in exploring the entry of materials into the liver cells. Many important substrates penetrate cell membranes by virtue of the presence of carrier-mediated membrane transport mechanisms (29). These mechanisms are specific, often even stereospecific. They exhibit saturation kinetics: with a rise substrate concentration, the rate of transfer does not rise proportionately; it reaches a maximum at some upper level. The proportional uptake of tracer falls with rise in bulk substrate concentration; this is the effect of saturation at the tracer level. Carrier-mediated transport mechanisms also characteristically exhibit two other properties: with related substrates, competitive inhibition of the membrane transfer process can usually be demonstrated, and under appropriate circumstances the phenomenon of counter-transport can be elicited.

Glucose transfer is an ideal process to explore in seeking evidence of a carrier-mediated transport process. The uptake of glucose by the liver is nonconcentrative. The intracellular concentration of free glucose in the liver is equal to the concomitant plasma concentration, as long as it is not substantially below the normal range

(5). The entry process has been demonstrated to be carrier mediated in other cells (29). Exploration of glucose entry into liver cells by the multiple-tracer approach provided an opportunity both for gathering data on the system (in particular, for determining whether nonlinearity and other characteristics of a membrane transport system were present) and for finding out whether a complete kinetic sinusoid-interstitium-cell model of exchange (12) could be fitted in satisfactory fashion to a relatively high-permeability set of data (18). A good fit had been obtained to a set of outflow curves for tracer rubidium (12), but these represented an easier domain in the modeling; in fact they approached the ideal isolated throughput-component Crone case. The permeability of the liver cell surface to the tracer rubidium was lower and the cell-entry process highly concentrative (so that tracer entering the cells had a long residence time and, conversely, returned slowly); thus early (and accessible) parts of the outflow profile consisted almost entirely of throughput components of tracer that had not entered the liver cells but otherwise had traveled to the outflow in the same manner as the interstitial or second-reference substance. Since glucose is not protein bound, no accessory features were expected to alter the process of label transfer.

Figure 2 illustrates a set of multiple-indicator dilution studies of hepatic glucose cell entry. Experiments with D-[^{3}H]glucose (the physiological stereoisomer) were carried out at underlying normal and high steady-state glucose concentrations and in the presence of the competitive inhibitor phlorizin. Evidence for a stereoisomeric effect was sought with L-[^{3}H]glucose (the nonphysiological isomer) at normal underlying steady-state glucose concentrations.

The experiments were carried out in an anesthetized dog. In this species the time of glucose equilibration between plasma and red cells is ~1 day (25). The tracer glucose was added to the injection mixture just prior to its use. Because the tracer is excluded from red cells during the experiment, the appropriate second reference was a low-molecular-weight interstitial material excluded from the red cells (labeled sucrose was used).

The labeled sucrose curves in Fig. 2 are related to the labeled red cell curves in the manner expected for flow-limited distribution: the outflow appearance is delayed, the curve rises to a later and lower peak, and the downslope decays more slowly. The shapes of the labeled glucose curves change progressively as the conditions of the experiment change. In the upper left-hand panel, where the glucose level was normal, the labeled glucose curve begins to rise at the same time as that of the labeled sucrose, but the increase is much slower; the curve reaches a later peak that is substantially lower than that for sucrose and then falls slowly. Model analysis of the data resolves a throughput component (shaded area), which otherwise would have remained hidden. In the upper right-hand panel, where the glucose levels are quite high, the labeled glucose curve assumes a more squared-off shape, rising relatively quickly to a prolonged low and flattened peak, with an ultimate slow decay. The resolved throughput component is larger but not yet visible as a separate entity. Intuitively, one could place more confidence in the model analysis if the throughput component of the curve could be made to become an

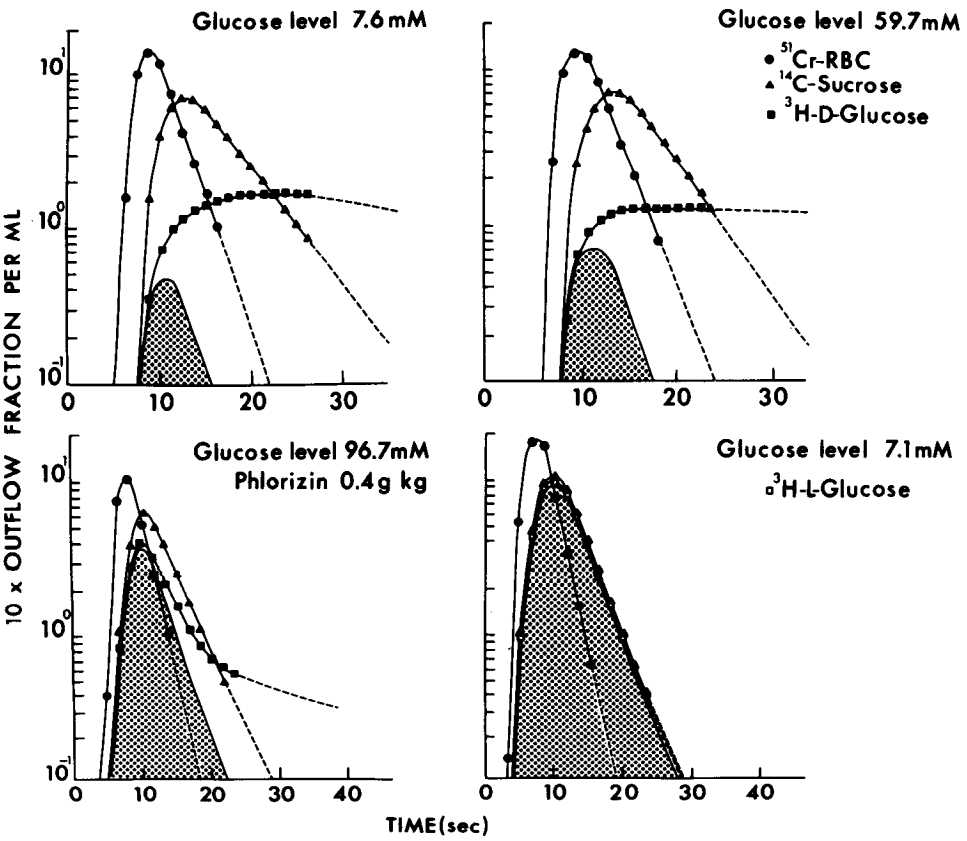

FIG. 2. Labeled glucose multiple-indicator dilution experiments. Ordinate scales are logarithmic. Computed throughput components have been shaded in each panel.

easily recognizable and separable component at the experimental level. This happens in the lower left-hand panel, after administration of the competitive inhibitor phlorizin. An early peak emerges from the D-glucose curve, related to and contained within the overlying sucrose reference curve; the analysis shows that this is the throughput component. The effect is even more dramatic for the nonphysiological stereoisomer L-glucose (lower right-hand panel). The curve closely approaches that of the second reference, the labeled sucrose curve. Very little of the label enters the liver cells; virtually all of the observable part of the curve is a throughput component.

The modeling not only resolved the throughput components from the labeled glucose profiles, but it also provided good fits to the curves as a whole (18) and, with this, gave optimized estimates of influx and efflux coefficients with no evidence of sequestration. Table 1 presents the forms of these coefficients (their physical equivalents). Each has the form of a permeability-surface product divided by the volume of the compartment from which the flux is originating. The influx coefficient is $P'_{in}S/[(1 + \gamma)V_p]$, where P'_{in} is an influx permeability equivalent, S is the surface area of the liver cells, V_p is the sinusoidal plasma volume, and γ is the ratio of accessible interstitial to plasma spaces, so that $(1 + \gamma)V_p$ represents the whole of the accessible space outside the liver cells, an expanded plasma volume. The efflux coefficient is $P'_{out}S/V_{cell}$, where P'_{out} is an efflux permeability equivalent and V_{cell} is the volume of the liver cells.

The overall pattern of change in the influx and efflux coefficients with change in the underlying glucose concentration is presented in Fig. 3. With increase in the plasma glucose concentration, both decrease in parallel. This systematic decrease in the coefficients with increase in the bulk glucose concentration indicates a saturation effect. It can be fitted in the following fashion. The bulk or parent glucose concentration in the system is defined as u_{par}. Then we would expect

$$(\text{flux coefficient})\ u_{par} = \frac{V_{max}\ u_{par}}{u_{par} + K_m}$$

where V_{max} is the maximal transport rate, referred to the appropriate volume, and K_m is a Michaelis-type constant for the transfer process. Then

$$\text{flux coefficient} = \frac{V_{max}}{u_{par} + K_m}$$

When this relation is fitted to the data in Fig. 3, a common K_m value is found for both influx and efflux, a glucose concentration of 122 mM. Because in this system the membrane transfer process is known to be nonconcentrative, we may conclude that $P'_{in} = P'_{out}$. The ratio of the influx coefficient to the efflux coefficient is then equal to the ratio of the cellular space to the expanded plasma volume. The maximum glucose transport rate, referred to the cellular volume, is 0.028 ml·s^{-1}·(ml intracellular space)$^{-1}$. The value is high; it is of the order of three times the transport maximum for D-glucose in human erythrocytes (29).

The other phenomena characteristic of a carrier-mediated transport process are also present. D-Galactose acts as a competitive inhibitor of D-glucose transport. Increasing its concentration, at normal glucose levels, causes progressive diminution in the rate of D-glucose label entry into the liver cells (18). To demonstrate the countertransport of labeled D-glucose in vivo, labeled D-glucose and labeled sucrose were allowed to equilibrate in the system. A high concentration infusion of unlabeled glucose was then begun, and outflow tracer concentrations were recorded. A base-line dilution effect occurred. Efflux of water from the liver cells in response to the hypertonic glucose infusion reduced the outflow concentration of labeled sucrose. Simultaneously the outflow concentration of labeled glucose rose rather than fell; a counterflush of label activity occurred (18). The data can be construed to document the presence of a mobile carrier transport process for D-glucose in the liver cell membranes (29).

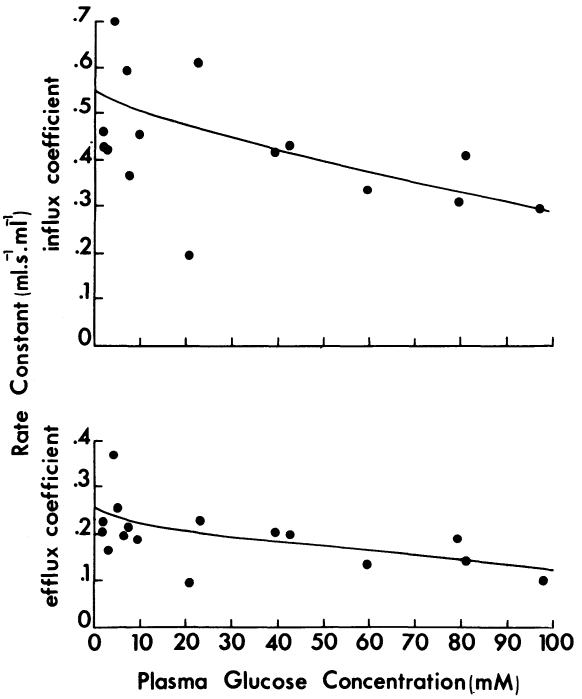

FIG. 3. Changes in flux coefficients for tracer D-glucose with change in underlying plasma glucose concentration. Continuous lines correspond to relations fitted through the points.

Intracellular Sequestration Behind a Barrier

For most important metabolic substrates, the cell membrane functions in a barrier-limiting fashion. The membrane is not usually freely permeable to the substrate so that, with consumption occurring inside the cells, the cell membrane begins to function in a limiting fashion. A concentration drop, from outside to inside, occurs across the surface. At the same time, downstream cells receive only the material that has escaped sequestration upstream and later moved downstream. As a consequence, an axial gradient in bulk concentration develops. Concomitantly, in a simultaneously performed tracer experiment, a proportion of the tracer that has entered the liver cells will be irreversibly removed from

the system; tracer will be recovered at the outflow in proportion to bulk (13).

D-Galactose, a hexose that is removed from the circulation and sequestered by the liver, is an ideal substance to compare to glucose. When the plasma bulk galactose level is high, the bulk removal rate is constant; so long as the hepatic blood flow is constant, a constant arterial-hepatic vein concentration difference results. When the concentration is low (less than ~1.7 mM), the steady-state extraction becomes quite high and the blood is almost cleared of galactose during its transit through the liver. The extraction of galactose is so large in this lower range (avg 88% in normal human) that its constant low-level infusion has been used to estimate hepatic blood flow (27, 28). Net removal of galactose may be used as a prototype for removal of other materials. Two sets of phenomena underlie gross observations of uptake: *1*) a process of membrane carrier transport, which subserves the entry of galactose into and its exit from liver cells; and *2*) a metabolic removal process, which in this case is phosphorylation by galactokinase, with the production of galactose 1-phosphate, a compound that cannot exit through the liver cell membrane. This compound is ordinarily rapidly converted to glucose 1-phosphate by the enzyme galactose-1-phosphate uridylyltransferase [the enzyme usually deficient in galactosemia (23)]; with further metabolism, this is utilized either for glycogen synthesis or as a source for intracellular glucose production.

Figure 4 shows the outflow profiles from a set of D-[^{3}H]galactose indicator dilution experiments for low (0.3 mM), intermediate (12.5 mM), and high (17.5 mM) input galactose concentrations and from an experiment in which the nonphysiological stereoisomer L-galactose was used as the molecular probe. At the lowest galactose concentration, the D-galactose tracer curve consists of a low-in-magnitude early peak (included under the labeled sucrose curve) followed by an abbreviated, low-in-magnitude tailing. Only a small proportion of the total injected galactose activity emerges at the outflow. At the intermediate galactose concentration, the early part of the curve increases in magnitude and blends with a later and much increased tailing, which now crosses the downslope of the sucrose curve relatively early. More of the activity emerges at the outflow. At the highest galactose concentration, the curve appears to resolve into two components: an early and distinguishably larger peak contained within the sucrose curve and a prolonged component with a later, low-in-magnitude tailing. The proportional net uptake of the label becomes small at this highest concentration (13).

The modeling developed for the glucose case was extended by adding an irreversible sequestration of label within the liver cell compartment (11, 13). A sequestration coefficient (Table 1, k_3'/V_{cell}), with the dimensions milliliters per second per milliliter, was used to describe the removal process. The resultant outflow modeling was then fitted to the data. The analysis provided throughput

TABLE 1. *Definitions of influx, efflux, and sequestration coefficients*

Coefficient	Physical Equivalent
Influx	$\frac{P'_{in}\,S}{(1+\gamma)V_{pl}}$
Efflux	$\frac{P'_{out}\,S}{V_{cell}}$
Sequestration	$\frac{k_3'}{V_{cell}}$

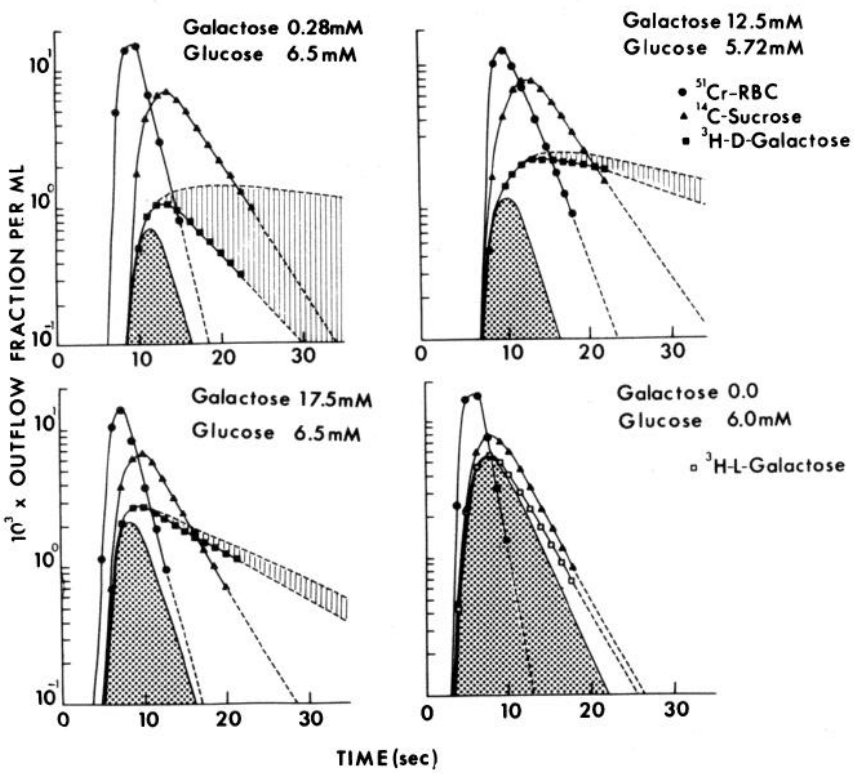

FIG. 4. Labeled galactose multiple-indicator dilution curves. Ordinate scales are logarithmic. Throughput components have been emphasized by dotted shading; differences between observed curves and profiles expected if there was no sequestration are highlighted by vertically hatched shading.

and returning components; in the fitted solution, when the sequestration coefficient was set equal to zero, computation also gave the form the galactose curve would have had if none of the tracer had been sequestered—that is, if all of it had returned to the circulation. The resolved throughput components have been added to Fig. 4. They increase in magnitude with increase in the bulk parent galactose concentration, reflecting saturation of the transfer process in the hepatocyte cell membrane. The membrane saturation is most evident in the transition from the intermediate to the high galactose concentrations. Stereoisomeric preference of the membrane transfer mechanism becomes clear in the L-galactose panel; the throughput component becomes very large indeed. Cell entry of the nonphysiological L-galactose tracer is quite slow. The sequestration process changes the outflow from that projected by setting the sequestration coefficient equal to zero in the final best fit to that observed at the outflow. The difference between the two curves in Fig. 4 has been emphasized with hatched shading; this documents the relative magnitude of the metabolic sequestration effect in the various cases. An increase in the magnitude of the effect with time is clearly evident in each panel; the sequestration effect is very large, far out on the downslope of the curve. It is also clear that the enzymic process underlying the sequestration saturates at much lower concentration levels than the carrier-mediated membrane transport process. Thus net uptake (the result of the sequestration process) diminishes most rapidly in the transition from the low to the intermediate galactose concentration, whereas saturation of the entry process is most evident in the transition from the intermediate to the high concentration range. The modeling provided good fits to the data; no systematic deviations from the data were evident in the fit.

The enzymatic process underlying galactose sequestration is characterized by Michaelis-Menten kinetics (8), and thus the sequestration coefficient is expected to diminish with saturation, in a fashion analogous to the decrease in influx and efflux coefficients, with saturation of the membrane uptake process. The change in all three coefficients, with change in the input galactose concentrations, is illustrated in Fig. 5. The sequestration coefficient saturates very quickly over a range of concentrations across which the influx and efflux coefficients change slowly. Substantial saturation of influx and efflux coefficients occurs only over the higher concentration range. When the derived values for the coefficients were related to the input plasma galactose concentrations, the K_m value for the influx coefficient was 28.6 mM and that for the sequestration process was 1.3 mM. The ratio between galactose influx and efflux coefficients (the ratio of the cellular space to the expanded plasma volume) was almost identical to that found in the glucose experiments (i.e., the galactose transport process at the cell membrane can also be assumed to be nonconcentrative). This approach to the analysis of the data (i.e., relating parameter values to input concentrations) neglects both the axial concentration gradients expected in the sinusoids and the concentration drop across the sinusoidal face of the hepatocytes. Another approach, which considers these

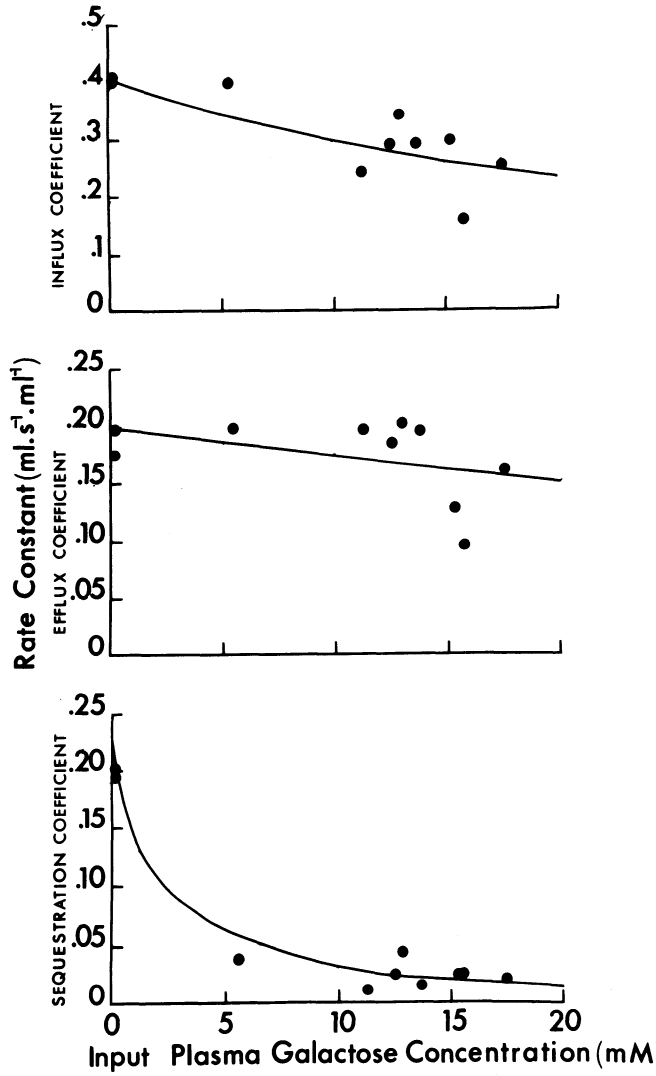

FIG. 5. Changes in flux and sequestration coefficients for tracer D-galactose with change in underlying plasma galactose concentration. Continuous lines correspond to relations fitted through points.

phenomena, will be considered after the characteristics of the space profiles are explored in more detail.

The cellular mechanism for galactose entry appears to fulfill the criteria for a carrier-mediated transport mechanism. The data demonstrate that the mechanism is stereospecific and saturates with increasing bulk galactose concentration. Glucose infusion produces a competitive inhibitory effect that rises progressively with plasma glucose concentration (13); phlorizin, which binds to the membrane, also inhibits the transport. No test for countertransport has been applied, since the intracellular removal of tracer would be expected to blunt this kind of response.

The presence of underlying steady-state longitudinal (i.e., axial) concentration profiles brings into focus several questions. To what bulk concentrations should the processes of influx, efflux, and sequestration be related? Can one find appropriate values with which to define more closely the set of concentration-dependent relations shown above? The answers are complex; the areas in which some of the answers lie have slowly become clear

but the details remain a challenge. The analyses that have been done lead to an additional question: will coefficient values in the single experiment change with concentration across a range small enough that the values within the experiment can be considered constant? In dealing with these questions one needs to gain insight into the processes involved and to arrive at a viewpoint allowing analyses of a set of data.

These questions can be examined at two levels: by analysis of the single experiment and by analysis of the aggregate data obtained from a group of experiments carried out across a wide range of input concentrations. The initial modeling developed for the analysis of the single experiment contains an intrinsic assumption of linearity in the handling of both tracer and bulk (13). With this assumption one can extrapolate from the rate constants obtained by analysis of the tracer experiment to an accompanying steady-state bulk concentration behavior (by examining the concentration step response of the system at long time). The predicted steady-state expressions (13) for the underlying concentration profiles of parent unlabeled material in the sinusoid u_{par} and liver cells z_{par} are

$$u_{par}(x) = u_{par}(0) \exp\left[-\frac{k_1\theta k_3}{k_1 + k_3}\frac{x}{W}\right]$$

and

$$z_{par}(x) = \frac{k_1}{k_2 + k_3} u_{par}(x)$$

where k_1 and k_2 are permeability-surface products per unit cellular volume, k_3 is the rate constant for irreversible removal per unit cellular volume, θ is the ratio of cellular to sinusoidal plasma spaces, x is the distance along the sinusoid, and W is the velocity of sinusoidal flow. Parallel exponentially declining profiles are predicted, with a step-down in concentration across the cell membrane, so that intracellular concentrations at each point are lower than plasma sinusoidal concentrations. Examination indicates that the space average value of the declining exponential profile is the logarithmic average concentration ([difference between input and output concentrations]/[difference between natural logarithms of input and output concentrations]). In this linear system, the value to which it is appropriate to relate the influx coefficient along each sinusoid is the logarithmic average sinusoidal unlabeled bulk concentration, and the value appropriate for relation to the efflux and sequestration coefficients is the parallel lower logarithmic average cellular unlabeled bulk concentration (14).

The assumption infers that the values for the rate constants do not change within the single experiment as a function of the range of underlying bulk concentrations encountered. At the appropriate level the assumption of linearity is thus really one of piecewise linearity over the range of concentrations encountered within the single experiment. Because in the single experiment the predicted bulk and observed tracer outflow recoveries will match, a set of steady-state unlabeled bulk exponential profiles will implicitly be fitted between common input and predicted output concentrations. Over the whole sinusoidal array, the weighted average of the set of predicted logarithmic concentration averages is the logarithmic average calculated by use of the mixed hepatic venous outflow concentrations (16). Hence we can relate the fitted rate constants to logarithmic average bulk concentrations calculated from common input and mixed venous outflow concentrations. We can continue our analysis of the data underlying Fig. 5, relating the influx coefficient to the logarithmic average sinusoidal concentration and the efflux and sequestration coefficients to the calculated logarithmic average intracellular concentration. The K_m for the process of galactose membrane transfer then decreases from 28.5 mM to a newly calculated value of 22.5 mM (this becomes 20.5 mM when the effect of the underlying normally competing glucose is accounted for), and the K_m for the intracellular enzymic sequestration process decreases from 1.3 to 0.4 mM. The latter change is large; the effect of the step-down in concentration across the cell membrane is particularly significant. The new estimate of K_m for sequestration is of the same order as the K_m determined for galactokinase from pig liver (3, 8, 24). The calculated maximal intracellular sequestration rate is only 0.038 times the maximal rate predicted for the membrane trasnsport mechanism.

This approach to the analysis provides a much closer approximation to the true values of the characteristic parameters of both the membrane carrier transport mechanism and the intracellular enzymic sequestration mechanism. A more complete analysis of this kind of system would demand a higher level of generality. To achieve this, the nonlinearity of the transport mechanism and the nonlinearity of the intracellular sequestration mechanism would both necessarily be incorporated in the formulations. The equations for both the underlying steady-state behavior of unlabeled substrate and for the transient behavior of tracer would be written, and these equations, incorporating the nonlinearity at each level, would then be solved together. These demands are idealistic and undoubtedly will be difficult to fulfill; in any case they may not be very useful for single experiments because the underlying substrate concentration will not sweep through a wide enough range with respect to the $K_m$values to provide data sensitive to the parameters being ascertained. Experiments at different concentrations within the same organ will be necessary if values unique to that particular organ are to be determined. The area does hold promise; some limited attempts have already been successful. Analytical solutions for steady-state bulk profiles, when enzymic sequestration is occurring without a barrier (i.e., in the flow-limited case), have been shown to vary from exponential at the lower concentration to a low-slope, linearly decreasing concentration at the higher extreme (4, 14), and a similar evolution of sinusoidal and cellular profiles has been found for the situation in which a barrier-limiting, cell-entry mechanism can be treated as linear over the saturation range of an enzymic sequestration mechanism (14). Incorporation of the nonlinear steady-state behavior in the equations describing transient tracer behavior has been possible in these two cases (14). The logarithmic average

has again been demonstrated to be useful here; its utility extends not only over the lower concentration range (where the profiles are exponential) but also up into the higher concentration range (where steady-state profiles slowly decrease in a linear fashion) (4, 14).

The predicted profiles leave their imprint at a morphological level. Autoradiography showed that labeled galactose was incorporated into intracellular glycogen in high concentration in periportal cells and in low concentration in the regions near the terminal hepatic venules 2 min after intravenous tracer administration (13). Removal of bile salts, which are taken up from the blood and excreted in canalicular bile (which flows countercurrent to the blood), would also be expected to create a gradient. It has not been possible to visualize this with conventional bile salts because these are highly water soluble and are extracted from tissues during fixation and processing. However, Jones et al. (22) have found a bile salt analogue, iodinated cholylglycylhistamine, that will cross-link to protein through the imidazole ring during glutaraldehyde fixation, so that it is not significantly extracted from tissue during histological processing. A distinct lobular gradient in the acinar concentration of this labeled compound was recorded by radioautography. Gumucio et al. (21) explored the cellular uptake of fluorescent compounds excreted in bile; with progressive loading, they were able to visualize the expected flattening of the gradient and recruitment of downstream hepatocytes, with rise in input concentration.

The modeling of outflow tracer profiles previously brought forward the prediction of the presence of underlying unlabeled bulk profiles (13). The more detailed investigation of these can now be expected in turn to affect the modeling of tracer handling, as more experimental details are revealed.

Effect of Protein Binding on Hepatic Uptake Processes

The development of a method enabling us to separate transfer processes at the liver cell surface from processes that sequester label either metabolically or by biliary secretion makes it possible to ask new questions concerning the details of these processes. In particular one can begin to examine how the uptake of materials by the liver cells is affected by binding to protein on either side of the cell surface. Bilirubin is archetypal for this group of substances. It is tightly bound to albumin in plasma and is taken up in net fashion by the liver for biliary excretion. A proportion of the bilirubin in plasma but not albumin (10) is transferred across the cell membrane into the liver cell where intracellularly it binds primarily to ligandin (glutathione *S*-transferase B) and, to a lesser extent, to other glutathione *S*-transferases and Z protein (2).

Wolkoff et al. (30) examined the effect of the intracellular binding proteins on the uptake process. They obtained a set of multiple-indicator dilution curves in the isolated nonrecirculating perfused rat liver, utilizing livers from normal animals and from animals in which the ligandin levels were increased by phenobarbital treatment and thyroidectomy. The experiments were carried out in the absence of bilirubin load, so that a greater proportion of the bilirubin tracer would enter the liver cells. The theoretical background developed for the analysis of experimental data needs modification under this set of circumstances. Binding to a protein will be expected to reduce the availability of tracer (and bulk) to the membrane. Bile acid uptake by isolated hepatocytes, for instance, is suppressed by albumin, which binds this substrate (1). To account for the protein binding on either side of the membrane, define a set of binding coefficients (r_p and r_c) that detail the effect of protein binding in plasma and cell space, respectively. If free concentrations are considered to mediate the transfer across the membrane, r_p and r_c will be defined as the ratio of total to free concentrations in the respective phases. The influx coefficient will now be divided by r_p, and the new efflux and sequestration coefficients, by r_c. Each coefficient will decrease as the concentration of the corresponding protein increases and will increase whenever competitors decrease the average affinity of the protein for substrate; when there is no binding, each will be unity. In the formulation outlined here, neither the rate of unbinding nor of binding is assumed to be limiting. If they were, the equilibrium ratios between total and free concentrations, described by the coefficients r_p and r_c, would not apply to the downstream tracer situation, either in sinusoid or in cell. Assuming that this does not occur, we find (Table 1) that the ratio of the coefficients at the membrane is

$$\frac{\text{influx coefficient}}{\text{efflux coefficient}} = \frac{P'_{in}}{P'_{out}} \frac{V_{cell}}{(1+\gamma)V_{pl}} \frac{r_c}{r_p}$$

The flux ratio now contains the term r_c/r_p. In the set of experiments to be examined, increase in ligandin concentrations would be expected to directly increase r_c and hence the ratio r_c/r_p.

Outflow patterns from a typical set of indicator dilution experiments with labeled bilirubin, together with the analyses of these curves, are illustrated in Fig. 6. Only the curves for labeled albumin and labeled bilirubin are shown; those for the vascular reference (labeled red cells) are omitted for the sake of clarity. In the normal animal, the bilirubin curve progressively diverges from the albumin curve on the semilogarithmic plot until the middle downslope and then begins to approach the albumin curve and would have crossed it if the sampling had been continued for a longer time. In contrast, in the animal with elevated ligandin levels, the late approach to the albumin curve is not evident on the semilogarithmic plot. The fitted components show how the curves differ. The two throughput components are quite similar when compared with their albumin reference curves, whereas the returning components are quite different. In the normal animal the returning component is large enough that the downslope of the bilirubin curve obviously approaches that for albumin; where this component is plotted separately (middle panel), it quantitatively dominates the outflow, late in time. The forms of the complete profiles and of the returning components, if no sequestration had occurred, are illustrated in the upper and middle panels, respectively. The difference

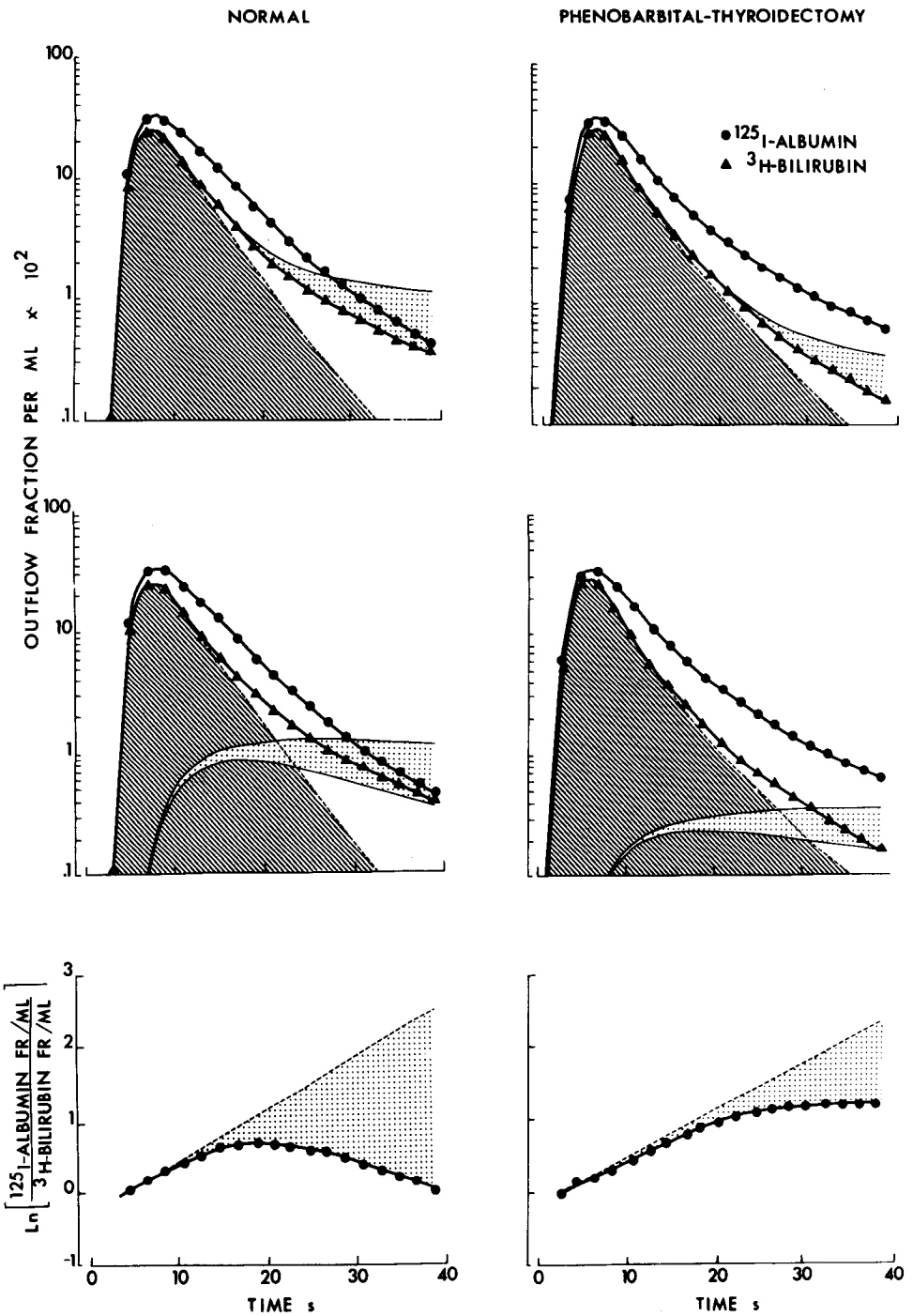

FIG. 6. Labeled bilirubin multiple-indicator dilution experiments. *Left-hand panels*: from a normal control animal; *right-hand panels*: from animal in which ligandin concentrations had been raised by phenobarbital pretreatment. Throughput components in upper and middle panels have been emphasized by hatched shading; in upper two panels, differences between profiles expected if there had been no sequestration and returning components are emphasized by dotted shading. Natural logarithm ratios are plotted in lower panels. From Wolkoff et al. (30).

between these and the observed profiles (emphasized by dotted shading) represents the net effect of the sequestration flux. In the phenobarbital-treated animal the second component is grossly reduced; the qualitative contribution of the returning component to the outflow profile is small, late in time. Even the second component predicted in the absence of sequestration is reduced. The log ratio plots in the lower panels demonstrate the dramatic difference between the two situations in a different manner.

The influx coefficients do not vary significantly between the groups, whereas the efflux coefficients vary inversely with the ligandin concentration (see Fig. 7). The sequestration coefficient does not change significantly with the ligandin concentration. The ratio of influx coefficient to efflux coefficient is illustrated as a function of the ligandin concentration in the lower panel of Fig. 7. This ratio, which will be expected to vary as r_c/r_p, increases directly with the ligandin concentration.

These studies demonstrate a decrease in the efflux of

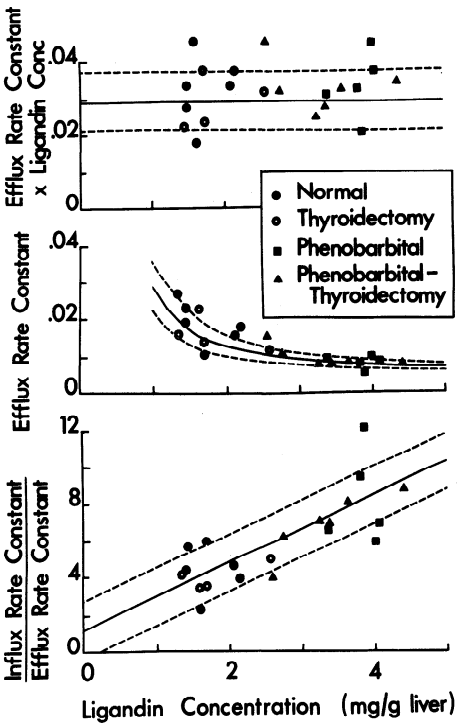

FIG. 7. Change in efflux coefficient and flux coefficient ratio with ligandin concentration. *Upper panel*: product (efflux rate constant times ligandin concentration) is plotted against ligandin concentration. *Solid line*, linear regression through data; *dashed lines*, SE of fit. Corresponding relation (an inverse variation of efflux coefficient with ligandin concentration) is mapped into middle panel. *Lower panel*: variation of ratio (influx coefficient/efflux coefficient), ratio of cellular space to expanded plasma space, is related to ligandin concentration. *Solid line*, linear regression indicating that space ratio increases with ligandin concentration (dashed lines again correspond to SE of fit). From Wolkoff et al. (30).

labeled bilirubin from the liver cell as the ligandin concentration is increased. This occurs because, with increased ligandin concentration, the effective space of distribution of tracer bilirubin in the liver cell is increased and, with this, the efflux diminishes. The indicator dilution approach has provided insight into the effects of the intracellular binding of bilirubin that could have been obtained in no other way. The effects of intracellular binding proteins will also be expected to vary with the kind of substrate being examined. Thus, whereas bilirubin binds to ligandin without transformation, ligandin serves as a glutathione transferase for sulfobromophthalein, converting it to the glutathione-conjugated form excreted in bile. Additional kinetic effects will be expected with this.

Conversely, changes in the concentration of albumin or its affinity for substrate will also be expected to affect uptake. Thus addition of albumin to the vascular perfusion medium will be expected to reduce uptake (interpretations having to do with a membrane albumin receptor will need to consider this effect in a quantitative fashion). Decrease in the affinity of albumin for a substrate, conversely, will be expected to increase its uptake. Such an effect has been observed in a set of labeled palmitate experiments (15). Infusion of α-bromopalmitate reduces the affinity of albumin for tracer palmitate (with the increase in the total amount of material bound, the tracer palmitate is progressively randomized to lower-affinity secondary albumin-binding sites); consequently the rate of uptake of tracer palmitate by the liver is increased.

Summary

The single injection, multiple-indicator dilution technique provides a systematically evolving way of particularizing the uptake and sequestration of materials by the liver. It permits definition of the limiting effect of the cellular membranes of the liver cells on cell entry and exit, and it provides a way of distinguishing and measuring intracellular metabolic sequestration effects. The approach provides a set of tools with an unparalleled potential for obtaining in vivo information on the disposition of metabolically important substrates.

I express my appreciation to the Medical Research Council of Canada and the Quebec Heart Foundation for their project support and thank Margaret Mulherin for typing the manuscript. Support has also been provided by a Career Investigator Award from the Medical Research Council of Canada.

Address for reprint requests: C. A. Goresky, University Medical Clinic, Montreal General Hospital, 1650 Cedar Ave., Montreal, Quebec H3G 1A4, Canada.

REFERENCES

1. ANWER, M. S., R. KROKER, AND D. HEGNER. Effect of albumin on bile acid uptake by isolated rat hepatocytes. Is there a common bile acid carrier? *Biochem. Biophys. Res. Commun.* 73: 63–71, 1976.
2. ARIAS, I. M., G. FLEISCHNER, R. KIRSCH, S. MISHKIN, AND Z. GATMAITAN. On the structure, regulation, and function of ligandin. In: *Glutathione: Metabolism and Functions*, edited by I. M. Arias and W. Jakoby. New York: Raven, 1976, p. 175–188.
3. BALLARD, F. J. Purification and properties of galactokinase from pig liver. *Biochem. J.* 98: 347–352, 1966.
4. BASS, L., S. KEIDING, K. WINKLER, AND N. TYGSTRUP. Enzymatic elimination of substrates flowing through the intact liver. *J. Theor. Biol.* 61: 393–409, 1976.
5. CAHILL, G. F., JR., J. ASHMORE, A. S. EARLE, AND S. ZOTTU. Glucose penetration into the liver. *Am. J. Physiol.* 192: 491–496, 1958.
6. CHINARD, F. P., G. J. VOSBURGH, AND T. ENNS. Transcapillary exchange of water and other substances in certain organs of the dog. *Am. J. Physiol.* 183: 221–234, 1955.
7. CRONE, C. Permeability of capillaries in various organs as determined by use of the 'indicator diffusion' method. *Acta Physiol. Scand.* 58: 292–305, 1963.
8. CUATRECASAS, P., AND S. SEGAL. Mammalian galactokinase. *J. Biol. Chem.* 240: 2382–2388, 1965.
9. GORESKY, C. A. A linear method for determining liver sinusoidal and extravascular volume. *Am. J. Physiol.* 204: 626–640, 1963.
10. GORESKY, C. A. The hepatic uptake process: its implications for bilirubin transport. In: *Jaundice*, edited by C. A. Goresky and M. M. Fisher. New York: Plenum, 1974, p. 159–174.
11. GORESKY, C. A. The modeling of tracer exchange and sequestration in the liver. *Federation Proc.* In press.
12. GORESKY, C. A., G. G. BACH, AND B. E. NADEAU. On the uptake of materials by the intact liver: the concentrative transport of rubidium-86. *J. Clin. Invest.* 52: 975–990, 1973.
13. GORESKY, C. A., G. G. BACH, AND B. E. NADEAU. On the uptake of materials by the intact liver: the transport and net removal of galactose. *J. Clin. Invest.* 52: 991–1009, 1973.
14. GORESKY, C. A., G. G. BACH, AND C. P. ROSE. Effects of saturating metabolic uptake on space profiles and tracer kinetics. *Am. J. Physiol.* 244 (*Gastrointest. Liver Physiol.* 7): G215–G232, 1983.
15. GORESKY, C. A., D. S. DALY, S. MISHKIN, AND I. M. ARIAS. Uptake of labeled palmitate by the liver: role of intracellular binding sites. *Am. J. Physiol.* 234 (*Endocrinol. Metab. Gastrointest. Physiol.* 3):

E542–E553, 1978.
16. GORESKY, C. A., E. R. GORDON, AND G. G. BACH. Uptake of monohydric alcohols by liver: demonstration of a shared enzymic space. *Am. J. Physiol.* 244 (*Gastrointest. Liver Physiol.* 7): G198–G214, 1983.
17. GORESKY, C. A., AND A. GROOM. Microcirculatory events in the liver and spleen. In: *Handbook of Physiology. Cardiovascular System*, edited by E. M. Renkin and C. Michel. Bethesda, MD: Am. Physiol. Soc. In press.
18. GORESKY, C. A., AND B. E. NADEAU. Uptake of materials by the intact liver: the exchange of glucose across the cell membranes. *J. Clin. Invest.* 53: 634–646, 1974.
19. GORESKY, C. A., AND C. P. ROSE. Blood-tissue exchange in liver and heart: the influence of heterogeneity of capillary transit times. *Federation Proc.* 36: 2629–2634, 1977.
20. GORESKY, C. A., W. H. ZIEGLER, AND G. G. BACH. Capillary exchange modeling: barrier-limited and flow-limited distribution. *Circ. Res.* 27: 739–764, 1970.
21. GUMUCIO, J. J., D. L. MILLER, M. D. KRAUSS, AND C. C. ZANOLLI. Transport of fluorescent compounds into hepatocytes and the resultant zonal labeling of the hepatic acinus in the rat. *Gastroenterology* 80: 639–646, 1981.
22. JONES, A. L., G. T. HRADEK, R. H. RENSTON, K. Y. WONG, G. KARLAGANIS, AND G. PAUMGARTNER. Audioradiographic evidence for hepatic lobular concentration gradient of bile acid derivative. *Am. J. Physiol.* 238 (*Gastrointest. Liver Physiol.* 1): G233–G237, 1980.
23. KALCKAR, H. M., E. P. ANDERSON, AND K. J. ISSELBACHER. Galactosemia, a congenital defect in nucleotide transferase. *Biochim. Biophys. Acta* 20: 262–268, 1956.
24. KEIDING, S., S. JOHANSEN, K. WINKLER, K. TONNESON, AND N. TYGSTRUP. Michaelis-Menten kinetics of galactose elimination by the isolated perfused pig liver. *Am. J. Physiol.* 230: 1302–1313, 1976.
25. LARIS, P. C. Permeability and utilization of glucose in mammalian erythrocytes. *J. Cell. Comp. Physiol.* 51: 273–307, 1958.
26. ROSE, C. P., AND C. A. GORESKY. Vasomotor control of transit time heterogeneity in the canine coronary circulation. *Circ. Res.* 39: 541–554, 1976.
27. TYGSTRUP, N., AND K. WINKLER. Kinetics of galactose elimination. *Acta Physiol. Scand.* 32: 354–362, 1954.
28. TYGSTRUP, N., AND K. WINKLER. Galactose blood clearance as a measure of hepatic blood flow. *Clin. Sci.* 17: 1–9, 1958.
29. WILBRANDT, W., AND TH. ROSENBERG. The concept of carrier transport and its corollaries in pharmacology. *Pharmacol. Rev.* 13: 109–184, 1961.
30. WOLKOFF, A. W., C. A. GORESKY, J. SELLIN, Z. GATMAITAN, AND I. M. ARIAS. Role of ligandin in the transfer of bilirubin from plasma into liver. *Am. J. Physiol.* 236 (*Endocrinol. Metab. Gastrointest. Physiol.* 5): E638–E648, 1979.